Segmented Block Copolyetheramides Based on Nylon 6 and Polyoxypropylene. II. Structure and Properties

YEONG CHOOL YU and WON HO JO*

Department of Fiber and Polymer Science, Seoul National University, Seoul 151-742, Korea

SYNOPSIS

Structure–property relationships of segmented block copolyetheramides based on nylon 6 and polyoxypropylene (POP) were investigated as a function of the compositions and block lengths of the hard and soft segments by using differential scanning calorimetry, dynamic mechanical analysis, FT-IR spectroscopy, wide angle x-ray diffractometry (WAXD), and tensile testing. The nylon 6–D4 copolymers with the shortest soft segment exhibited the two-phase structure of a crystalline nylon 6 phase and an amorphous phase composed of the hard and soft segments. Also they showed the tensile properties characteristic of a plasticized thermoplastic. On the other hand, the nylon 6–D20 and nylon 6–D40 copolymers exhibited the three-phase structure of a crystalline nylon 6 phase, an amorphous nylon 6-rich phase, and an amorphous POP-rich phase. The nylon 6–D20 copolymers had better elastic properties with the increase of soft segment content; however, the nylon 6–D40 copolymers with the longest soft segment showed a substantial reduction of the elongation at break due to lack of the crosslinking density. © 1995 John Wiley & Sons, Inc.

INTRODUCTION

Recently segmented block copolyetheramides composed of polyamide as a hard segment and polyether as a soft segment have been widely investigated as a thermoplastic elastomer (TPE) since they possess good solvent resistance and excellent low temperature properties.[1-8] In the previous study,[9] we synthesized various block copolyetheramides based on nylon 6 and polyoxypropylene (POP) with different block lengths of the hard and soft segments, and determined their compositions and block lengths. Nylon 6 was selected as a hard segment because of its good mechanical properties and good processability. The hard nylon 6 segments form crystallites of high melting temperature which can physically crosslink the non-crystallizable soft segments. The POP units as a soft segment were expected to yield superior low-temperature properties due to its non-crystallizability and glass transition temperature (T_g) of −60°C. Since the POP unit contains a methyl side group for every oxypropylene unit, it has a low dipole moment, weak dispersion forces, and a low tendency toward hydrogen bonding, becoming incompatible with the hard segments.[10] The variation of the block length and composition of the hard and soft segments may affect the microphase separation, the composition of each phase, and the crystallinity, resulting in the change of physical properties of the block copolymer.

It is our primary aim to investigate systematically the microstructure and physical properties of the nylon 6–POP block copolymers as a function of the composition and block lengths of the soft and hard segments.

EXPERIMENTAL

Materials

Nylon 6–POP block copolymers were synthesized by melt polymerization of caprolactam (CPL), polyoxypropylene diamines (POPD), and adipic acid at 240°C, as described in the preceding paper.[9] Their compositions and block lengths, which were

* To whom correspondence should be addressed.

Journal of Applied Polymer Science, Vol. 56, 895–904 (1995)
 CCC 0021-8995/95/080895-10

calculated from ^{1}H-NMR data and a statistical theory of Sorta and Melis,[11] are listed in Table I. In sample codes, D4, D20, and D40 stand for the D-400 (mol wt 462), D-2000 (mol wt 2104), and D-4000 (mol wt 4540) grades of POPD, respectively, and the number behind D4-, D20-, and D40- represents the POPD content in the feed of polymerization.

Preparation of Specimens

Test specimens for measurements of the differential scanning calorimetry (DSC), wide angle x-ray diffraction, and dynamic mechanical properties were compression-molded by a laboratory press equipped with a thermometer and a cavity for the circulation of cooling water. The sample was molded for 5 min at a temperature 10–20°C higher than the melting point of the sample under the pressure of 250 kg/cm^2. Then the sample was cooled at a rate of 20°C/min to 100°C, the pressure was released, and the sample was removed. The average thickness of specimens was 0.8 mm.

Specimens for the tensile testing were obtained by injection molding with the Mini-Max Molder (CS-183MMV, Custom Scientific Instruments, Inc., New Jersey). The molding was performed at a temperature 10–30°C higher than the melting point of the sample. The miniature dumbbell specimen, having a gauge length of 9.3 mm and diameter of 1.6 mm, was obtained.

Measurements

DSC

The DSC measurements were taken by using Du Pont 910S Thermal Analyzer at a heating rate of 20°C under a nitrogen atmosphere. The temperature scale and heat flow were calibrated by use of an indium standard. Sample weight was about 5 mg.

Dynamic Mechanical Analysis

The dynamic mechanical properties were measured with a torsional pendulum on a Rheometrics RMS 800. Test specimens were cut from melt-pressed films to 45 mm long, 12 mm wide, and 0.8 mm thick. Torsional response data were obtained at 10°C intervals, but in the major transition region of −70–60°C the data were obtained at 5°C intervals. The storage and loss moduli were analyzed at a constant frequency of 1 Hz.

FT-IR Spectroscopy

The specimens in film form were fabricated by melt casting on a slide glass or a KBr pellet. An FT-IR spectrum was obtained by use of a Bruker IFS 88 FT-IR spectrophotometer.

Wide Angle X-ray Diffractometry (WAXD)

WAXD measurement was carried out on a MAC MXP18AHF diffractometer equipped with a rotat-

Table I Nylon 6–POP Block Copolymers Used in This Study

Sample Code	CPL/POPD Feed Ratio	Copolymer Composition (Wt %)		Mol Wt of Segment (g/mol)	
		Soft Segment	Hard Segment	Soft Segment	Hard Segment
D4-10	100/10	12.9	87.1	588	3,630
D4-20	100/20	21.5	78.5	602	2,040
D4-40	100/40	36.2	63.8	636	1,070
D4-60	100/60	46.7	53.3	670	743
D4-80	100/80	55.6	44.4	712	555
D20-10	100/10	11.4	88.6	2,230	9,900
D20-20	100/20	20.7	79.3	2,240	6,330
D20-40	100/40	31.9	68.1	2,260	3,960
D20-60	100/60	41.8	48.2	2,300	2,660
D20-80	100/80	49.3	50.7	2,320	2,400
D40-10	100/10	10.0	90.0	4,660	12,860
D40-20	100/20	19.6	80.4	4,680	10,230
D40-40	100/40	32.4	67.6	4,710	6,240
D40-60	100/60	44.1	55.9	4,740	5,950
D40-80	100/80	50.9	49.1	4,770	3,400

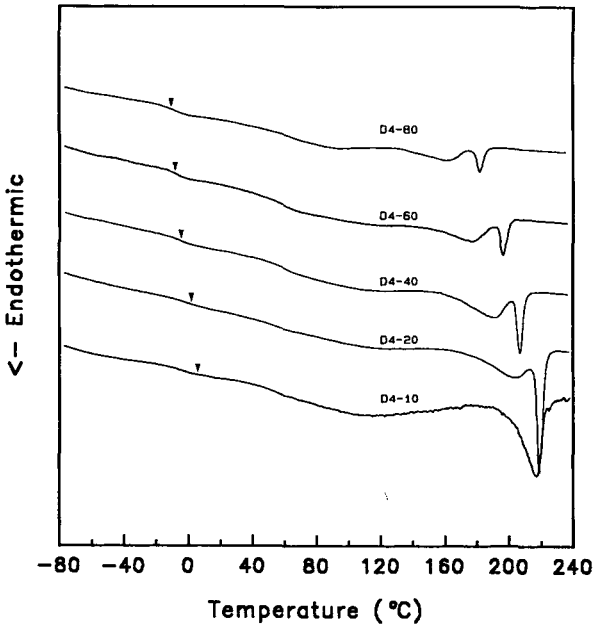

Figure 1 DSC thermograms of compression-molded nylon 6–D4 copolymers.

ing anode, pulse height analyzer, and step scanning device. The x-ray source was obtained at 45 kV and 200 mA and monochromatized to CuKα radiation with a graphite monochromator. WAXD diffractograms were obtained by scanning from 14° to 30° at a scan rate of 3°/min and a step angle of 0.02° in the reflection mode.

Tensile Properties

Uniaxial strain–stress curves were obtained at a cross-head speed of 2.5 mm/min by using an Instron 6022 testing machine.

RESULTS AND DISCUSSION

The phase separation of the nylon 6–POP block copolymers could lead to three phases of an amorphous POP-rich, an amorphous nylon 6-rich, and a crystalline nylon 6 phase. It is noteworthy that the POP unit is not crystallizable. DSC measurements were carried out to investigate the phase separation behavior and the variation of the crystal structure of the nylon 6–POP block copolymer with the composition and the block length of the hard and soft segments.

Figure 1 shows the DSC thermograms of the nylon 6–D4 block copolymers having the shortest soft segments. As the soft segment content increases, the melting temperature and the T_g decrease significantly. According to the explanation of Schmid and Droscher,[12] the melting point depression is attributed to the decrease of lamellar thickness due to the decrease of nylon 6 block length. The shifts of the T_g's indicate that the soft POP units are to some extent compatible with the rigid nylon 6 units in the amorphous region. The DSC thermograms of the nylon 6–D4 copolymers, except that of the D4–10 copolymer, exhibit two melting endothermic peaks. The appearance of the multiple melting endotherms has been explained by several mechanisms: melting of crystallites with different crystal structures (polymorphism),[13,14] melting of imperfect crystal followed by recrystallization and remelting,[15,16] and melting of crystalline lamellae with different thicknesses.[17,18] Figure 2 shows DSC thermograms of different heating rates for the D4–40 copolymer. The same results were obtained in the D4–20, D4–60, and D4–80 copolymer (not shown). In Figure 2, lower melting endotherms appear at constant temperatures regardless of heating rate, and the shape of two melting endotherms does not change with the variation of heating rate. This phenomenon implies that the multiple melting is caused by the presence of crystallites with different lamellar thickness.

Figure 3 shows the DSC thermograms of the nylon 6–D20 copolymers, which have longer soft block length than the nylon 6–D4 copolymers. As the soft segment content increases, the T_gs appear at nearly constant temperature corresponding to the T_g of the pure POP units, and melting endothermic peaks

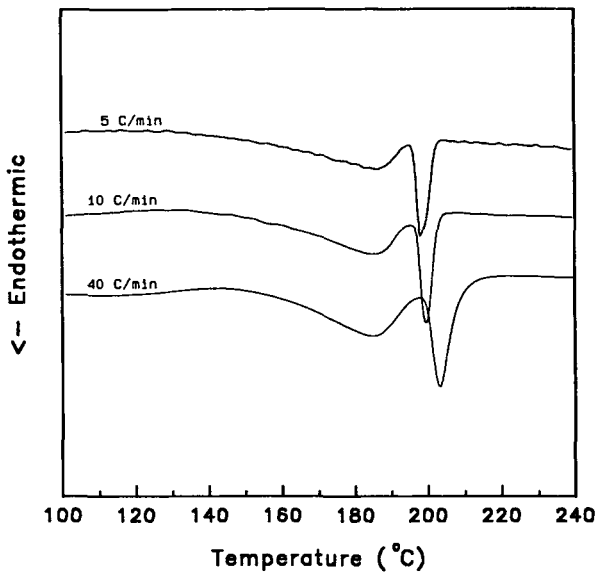

Figure 2 Dependence of melting endotherm of D4–40 copolymer on heating rate.

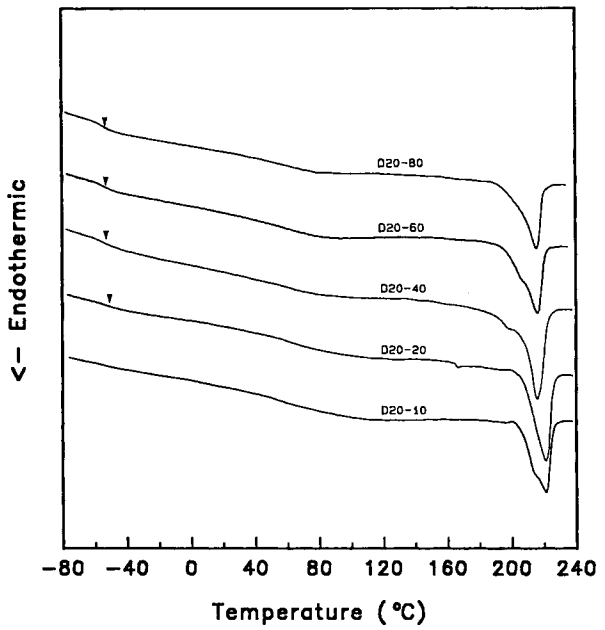

Figure 3 DSC thermograms of compression-molded nylon 6–D20 copolymers.

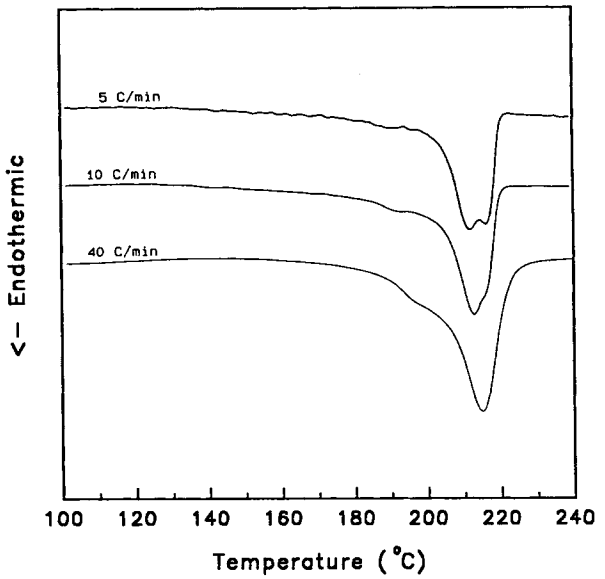

Figure 4 Dependence of melting endotherm of D20–40 copolymer on heating rate.

slightly shift to lower temperature. The T_g of the amorphous nylon 6 appears at 55°C, although it is somewhat ambiguous to explicitly determine its T_g due to broad transitions. Therefore it is presumed that the well-defined phase separation takes place in the amorphous region of the block copolymers. The melting endotherms of the nylon 6–D20 copolymers exhibit a shoulder. The origin of the shoulder is investigated by changing the heating rate as shown in Figure 4. Multiple melting endotherms are observed at a low scan rate, but only a single melting endotherm appears at a high heating rate. This result suggests that the appearance of the higher-temperature endotherm at a low scan rate is related to the recrystallization and remelting following the melting of the imperfect crystal during thermal analysis.

Figure 5 exhibits the DSC thermograms of the nylon 6–D40 copolymers having the longest soft segment. The same T_g for all compositions indicates that phase separation between the hard and soft domains takes place in the amorphous region.

The dynamic mechanical measurements were performed on compression-molded specimens in order to obtain information about the thermal transition behavior and the temperature dependence of mechanical properties of the block copolymers. Especially, the investigation of thermal transitions by dynamic mechanical analysis gives important information about the microstructure of the amorphous phase in block copolymers. Figure 6 shows the dynamic mechanical properties of the nylon 6 homopolymer as a function of the temperature. From the tan δ curve, a glass transition occurs at 50°C and a β relaxation due to the motion of five or six atoms along the main chain appears at −70°C.

Figures 7, 8, and 9 show the temperature dependence of the storage modulus (G'), loss modulus (G''), and tan δ for the nylon 6–D4, nylon 6–D20,

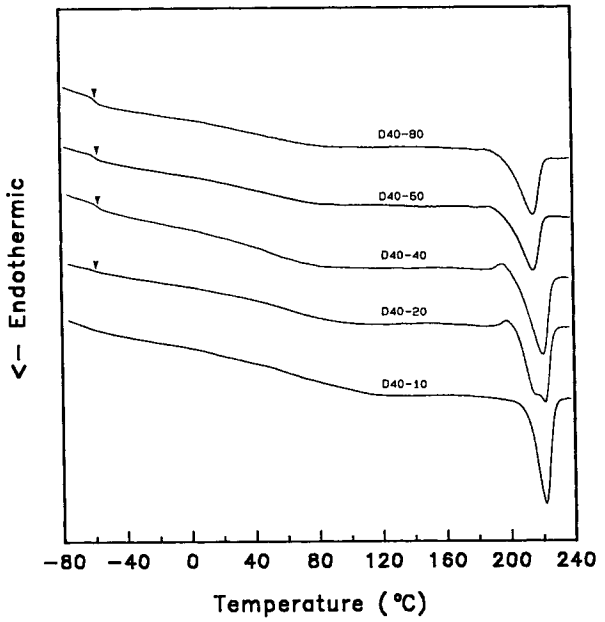

Figure 5 DSC thermograms of compression-molded nylon 6–D40 copolymers.

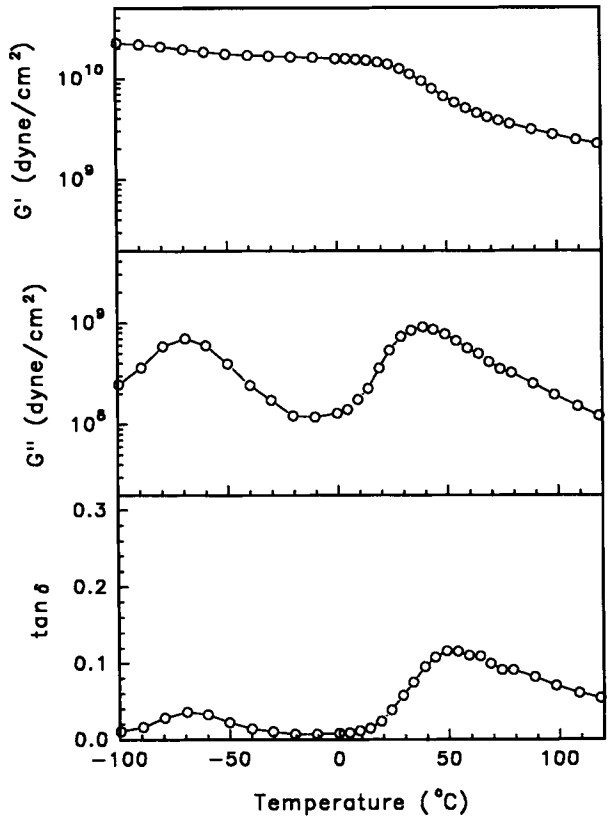

Figure 6 Temperature dependence of the dynamic mechanical properties of nylon 6 homopolymer.

and nylon 6–D40 copolymers, respectively. A substantial decrease in the storage modulus of the block copolymer corresponds to the transition from the brittle, glassy state to the elastic, rubbery state. Rubbery plateaus following the glass transition region of the soft domain are observed for all samples. An increase of soft segment content reduces the storage modulus in the rubbery plateau region. The rubbery moduli of the nylon 6–D20 and nylon 6–D40 copolymers are higher than that of the nylon 6–D4 copolymer at an equal content of the soft segment. According to the explanation of Miller et al.,[19] these higher rubbery moduli were ascribed to a high degree of phase separation and to an increase in the size and interconnectivity of the hard domains.

The dynamic loss modulus or tan δ is sensitive to various molecular motions, structural heterogeneities, and morphology of multiphase systems. The T_g generally corresponds to the temperature at the maximum of the loss modulus or tan δ. The magnitude of the mechanical loss peak represents the relative amount of the amorphous phase in the polymer undergoing the transition from the glass to the rubbery state. In Figure 7, single glass transition temperature of the nylon 6–D4 copolymer shifts to lower temperature with the increase of soft segment content. This trend is in good accordance with the DSC results for the nylon 6–D4 copolymers, suggesting that the rigid nylon 6 segments and the soft POP segments form one phase in the amorphous region. Also, the magnitude of the tan δ peak increases with the increase of soft segment content, indicating the development of the amorphous region. The mixing of the hard and soft segments suggests that the large amount of interface between soft and hard segments exists in the microstructure of the nylon 6–D4 copolymers and thus gives more chance to form hydrogen bonding between the ether group of the soft segment and the NH group of the hard segment. In Figures 8 and 9, there appear two T_gs of the nylon 6–D20 and nylon 6–D40 copolymers, −50−−60°C and 15–50°C. The lower T_gs remain almost constant regardless of the soft segment content while the magnitude of loss modulus or tan δ peak becomes higher with the increase of the soft segment content. On the other hand, as the soft segment content increases, the higher glass transition of the nylon 6–D20 copolymers shifts slightly to a lower

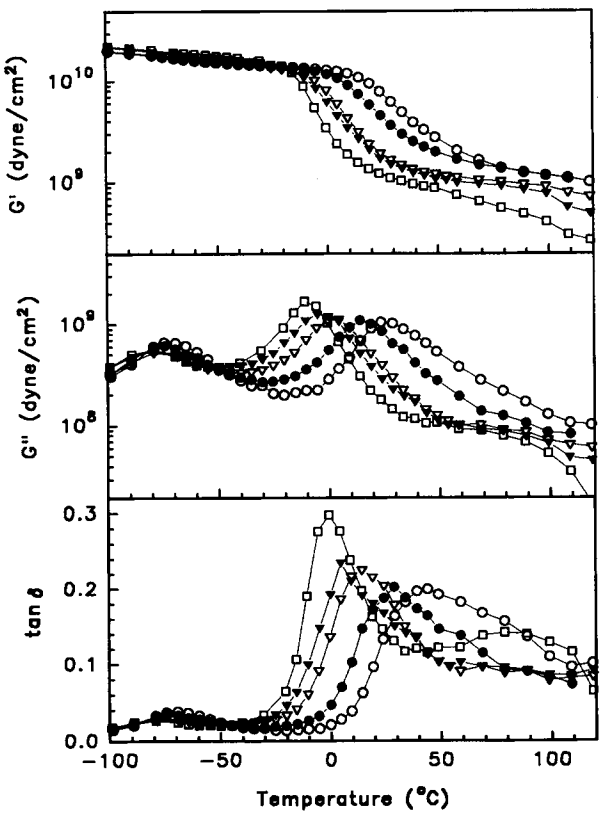

Figure 7 Temperature dependence of the dynamic mechanical properties of nylon 6–D4 copolymers: (○) D4–10, (●) D4–20, (▽) D4–40, (▼) D4–60, (□) D4–80.

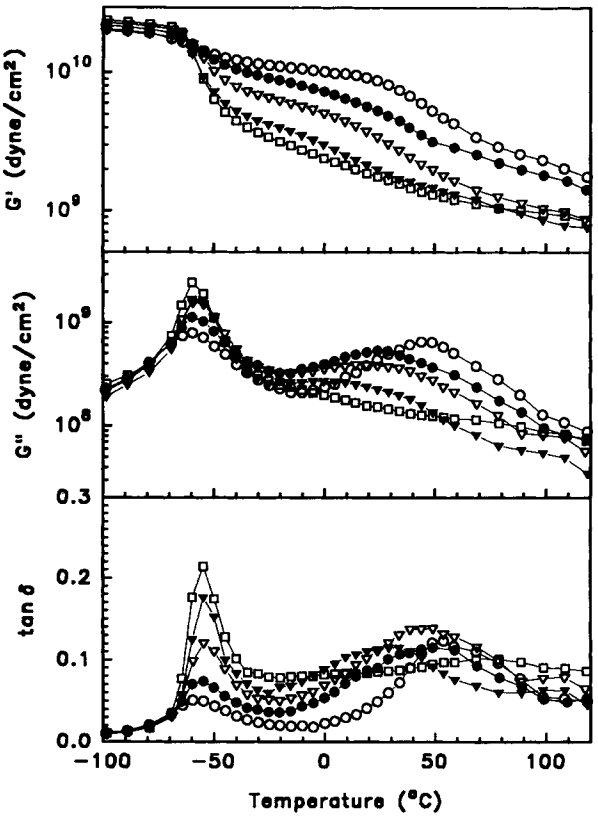

Figure 8 Temperature dependence of the dynamic mechanical properties of nylon 6–D20 copolymers: (○) D20–10, (●) D20–20, (△) D20–40, (▼) D20–60, (□) D20–80.

temperature while the magnitude decreases. These results represent that the microphase-separated structures exist in the amorphous region of the block copolymers. The invariance of lower transition temperatures implies that the hard segment is not nearly incorporated in the soft segment domain. The shift of higher transition temperatures is due to the incorporation of the soft segment into the amorphous region of the hard domain. The magnitudes of the two transition peaks of the nylon 6–D40 copolymers are higher than those of the nylon 6–D20 copolymers at the equal content of the soft segment, and the higher transition temperatures of the nylon 6–D40 copolymers remain almost constant. Therefore, it can be concluded that as the block length of the soft segment becomes longer, a better phase separation is induced, i.e., the purities of the hard and soft segment domains are enhanced.

FT-IR spectroscopy is very useful for studying the specific interaction between molecules and the structure of polymers. Skrovanek, Painter, and Coleman[20,21] reported that the IR absorptions attributed to ordered and disordered hydrogen-bonded amide groups are readily discerned since the C=O absorption is sensitive to conformation change through the dipole-dipole interaction. When the environment of the C=O group in simple amide is changed from complete association in the pure liquid or solid to complete dissociation in a nonpolar solvent, the C=O absorption shifts to higher frequency of 1680 cm^{-1}.[22] The absorption frequencies of the C=O bands in the nylon 6–POP copolymer were plotted against the soft segment content as shown in Figure 10. The C=O absorption frequency of nylon 6 homopolymer at room temperature is 1639 cm^{-1}. As the soft segment content increases, the C=O bands of the nylon 6–D4 copolymers shift progressively to a higher frequency while those of the nylon 6–D40 copolymers remain at almost the same positions. This result suggests that the hard and soft segments in the nylon 6–D4 copolymers are mixed to some extent at the molecular level; however, in the nylon 6–D40 copolymers the miscibility between the two segments is very low.

The crystal structure of the nylon 6 may be affected by the inclusion of a soft segment, though the POP unit does not participate in the crystal formation. From the observation of the multiple melt-

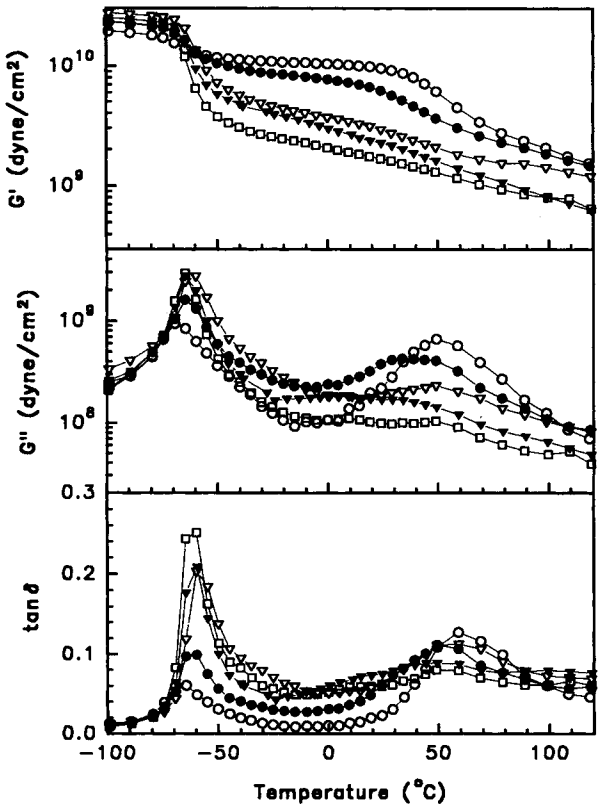

Figure 9 Temperature dependence of the dynamic mechanical properties of nylon 6–D40 copolymers: (○) D40–10, (●) D40–20, (△) D40–40, (▼) D40–60, (□) D40–80.

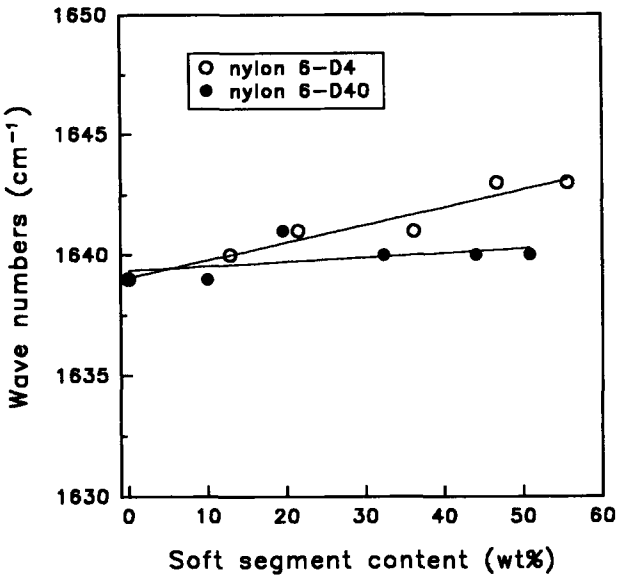

Figure 10 Frequency shift of the C=O absorption band as a function of the soft segment content.

ing endotherms in the DSC study, the nylon 6–D4 copolymers showed the possibility of the existence of polymorphism. Figure 11 shows the wide angle x-ray diffractograms for the compression-molded specimens of the nylon 6–D4 copolymers. The diffraction peaks of the nylon 6–D4 copolymers for all compositions demonstrate the presence of the α-crystal, which has two diffraction peaks at about 20° and 24° corresponding to the (200) and (002+202) reflections, respectively.[23] Therefore, it is presumed that the DSC multiple melting endotherms are attributed to the existence of the α-crystals with different thicknesses, not to the polymorphism. On the other hand, as the soft segment content increases, the full width half maxima (FWHM) of two peaks increase and the peak areas decrease, indicating the reduction of the crystal thickness and the degree of the crystallinity, respectively. The intensity ratio of the α-crystal, $I_{(002+202)}/I_{(200)}$, has been known as a measure of the rotation of the polymer chain.[23] When the antiparallel nylon 6 chains form hydrogen-bonded sheets, the intensity scattered by all atoms in the (002) planes becomes much higher than that scattered by the (200) planes with broader electron distribution. As the rotation of the polymer chain progresses, the electron density of the (002) planes approaches that of the (200) planes, and (002) and (200) reflections become nearly equal in intensity. The values of $I_{(002+202)}/I_{(200)}$ in the nylon 6–D4 copolymers were in the range of 0.85–0.95. This means that the rotation of the polymer chain occurs in the crystalline region of the nylon 6–D4 copolymer. Since the crystalline in polymers is very imperfect, its atoms tend to deviate from their ideal positions depending upon the thermal vibration, statistical disorder, and lattice imperfections. The results of the DSC and dynamic mechanical analysis explain that the nylon 6–D4 copolymers have a two-phase morphology composed of a crystalline domain and an amorphous domain arising from the homogeneous mixing of the nylon 6 and POP segments. In this system the introduction of the short POP units into the nylon 6 backbone may cause crystalline defects and statistical disorder like a random copolymer, giving rise to the rotation of the polymer chain.

The wide angle x-ray diffractograms of the nylon 6–D20 copolymers are shown in Figure 12. The diffraction peak of the γ-crystal is developed prominently at 2θ = 21.15°–21.42°. As discussed in the dynamic mechanical study, the amorphous hard domains in the nylon 6–D20 copolymers contain a small quantity of the soft segments. This result suggests that a considerable amount of the soft segments can be included in the melt state. These soft segments seem to be not completely removed from the hard domain during the crystallization by cooling and may constrain the formation of the α-crystals by a weak hydrogen bonding between the amide group of the nylon 6 segment and the ether group of the POP segment, resulting in the facilitation of the imperfect γ-crystal formation. The values of $I_{(002+202)}/I_{(200)}$ in the D20–10 and D20–40 copolymer

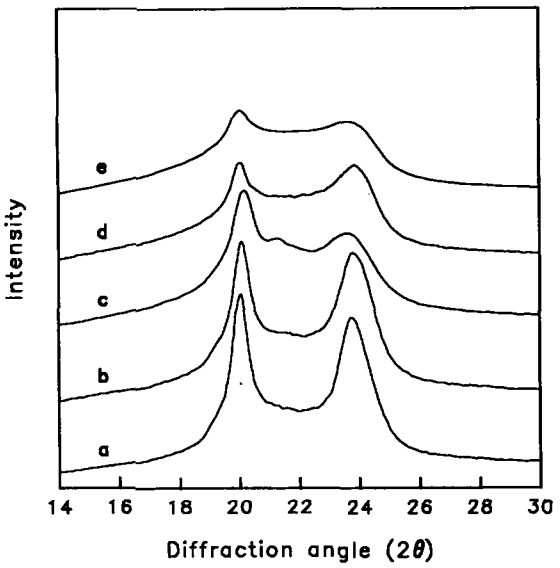

Figure 11 Wide angle x-ray diffractograms of nylon 6–D4 copolymers: (a) D4–10, (b) D4–20, (c) D4–40, (d) D4–60, (e) D4–80.

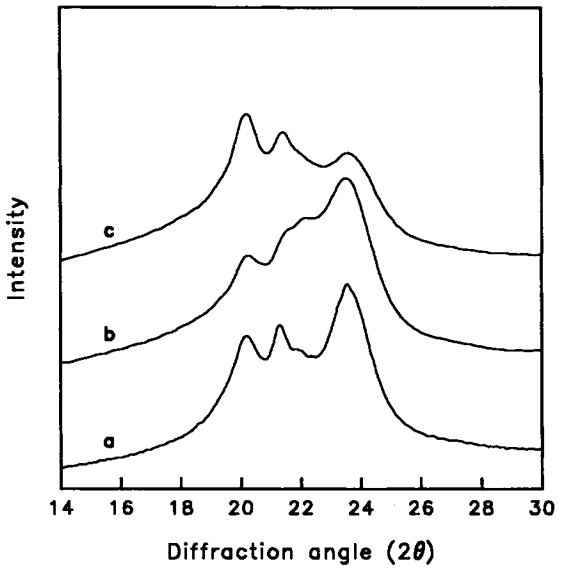

Figure 12 Wide angle x-ray diffractograms of nylon 6–D20 copolymers: (a) D20–10, (b) D20–40, (c) D20–80.

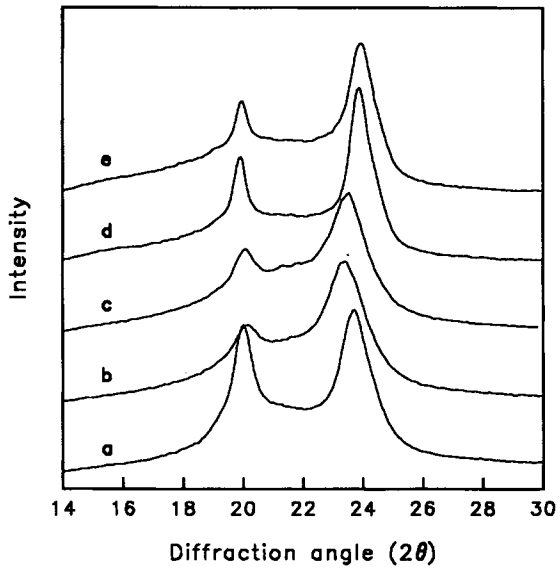

Figure 13 Wide angle x-ray diffractograms of nylon 6–D40 copolymers: (a) D40–10, (b) D40–20, (c) D40–40, (d) D40–60, (e) D40–80.

were 1.34 and 1.56, respectively, indicating that more perfect α-crystals are formed as compared with the nylon 6–D4 copolymers. However, the ratio of the D20–80 copolymer was 0.80. Accordingly, it is presumed that the inclusion of a larger amount of the POP segments into the hard domain induces the rotation of the polymer chain as well as the γ-crystal formation. The diffraction patterns of the nylon 6–D40 copolymers show the well-developed peaks of the α-crystals, as shown in Figure 13. The hard domains of the nylon 6–D40 copolymers include little soft segments in comparison with those of the nylon 6–D20 copolymers. The higher purity of the hard domains induces the formation of the α-crystals.

Generally, the strain–stress curve of a vulcanized elastomer does not show any yield point or distinct draw plateau region and shows low modulus.[24] However, the TPE consisting of the hard and soft domains exhibits somewhat different strain–stress patterns due to the existence of its thermoplastic character. According to Cella,[25] a typical strain–stress curve of the TPE can be characterized by three main regions of an initial high modulus region, a draw plateau region, and an ultimate elastic deformation region. The tensile behavior of a strained TPE depends mainly upon the size, shape, concentration, and interconnectivity of the hard domains, and the miscibility of the hard segments with the soft segments. Figure 14 shows the strain–stress curves for the nylon 6–D4 copolymers. As the hard segment content increases, both Young's modulus and the yield stress increase and the elongation at break decreases. All samples exhibit the yield point typical of thermoplastics. These results indicate that the nylon 6–D4 copolymers have tensile properties similar to a plasticized thermoplastic.

In Figure 15, the strain–stress curves of the D20–10 and D20–20 copolymer show the prominent yield points which are attributed to a high degree of interconnectivity of the hard domain. But the yield behavior disappears on the strain–stress curve of

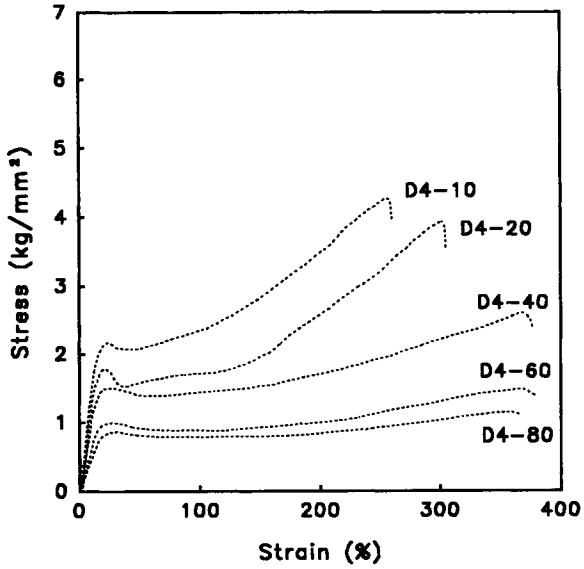

Figure 14 Strain–stress curves for nylon 6–D4 copolymers.

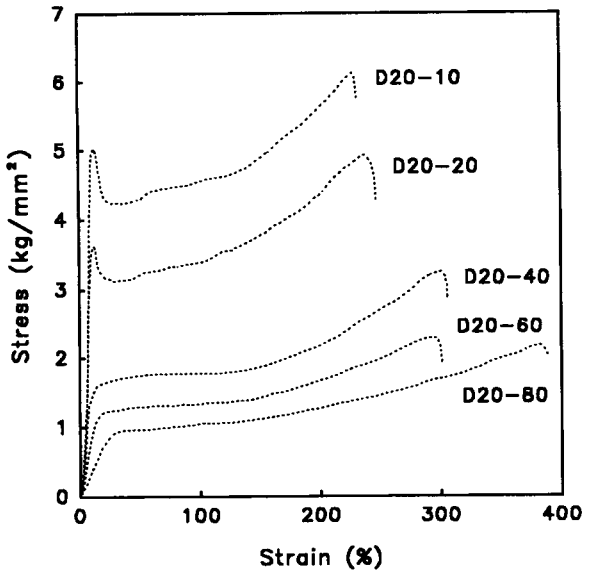

Figure 15 Strain–stress curves for nylon 6–D20 copolymers.

the D20–40 copolymer, which shows a typical pattern described by Cella.[25] This means that some morphological changes occur at the soft segment content of 32 wt %, i.e., the soft domain forms a continuous phase. Further increase of the soft segment content imparts better elastic properties to the polymer, since the polymers exhibit lower modulus, higher elongation at break, and the disappearance of the draw plateau region.

As shown in Figure 16, the nylon 6–D40 copolymers show the yield behavior even at the soft segment content of 32 wt %. This result indicates that the interconnectivity of the hard domain maintains at higher soft-segment content. Another characteristic feature in the nylon 6–D40 copolymers is the appearance of the wide range of the draw plateau region, in which extensive molecular orientation occurs. The range of the draw plateau region becomes wider as the soft-segment content increases. This phenomenon indicates that the occurrence of the draw plateau region is related to the orientation of the long soft segments. Above 32 wt % of the soft-segment content, the elongation at break decreases with increased soft-segment content. Especially, the D40–80 copolymer with a rather low modulus characteristic of lightly crosslinked rubber shows a substantial reduction of the elongation at break. This reduction can be considered to be ascribed to a lack of the crosslinking density appropriate to act as an elastomer. The nylon 6–D40 copolymers composed of large sizes of the hard and soft domains have small numbers of the crystalline domains to form a physical crosslink, compared with the nylon 6–D20 or nylon 6–D4 copolymers. The number of the crystalline domains reduces to a lower limiting value to bear the external force as the soft-segment content increases.

CONCLUSIONS

The microstructure and properties of the nylon 6–POP block copolymers were investigated as a function of the compositions and block lengths of the hard and soft segments. In the nylon 6–D4 block copolymers having the shortest soft segments, as the soft-segment content increases, their melting temperatures and glass transition temperatures decrease. The melting point depression is caused by the decrease of lamellar thickness as a consequence of the decrease of the nylon 6 block length. The shift of the glass transition temperature and the appearance of the single glass transition in the dynamic mechanical analysis indicate that the soft POP segments are compatible with the rigid nylon 6 segments in the amorphous region of the nylon 6–D4 copolymers. The observation of double melting peaks is attributed to the existence of the α-crystals with different thicknesses from the wide angle x-ray diffractometry. Consequently, the microstructures of the nylon 6–D4 copolymers are composed of the two-phase structure of a crystalline nylon 6 phase and an amorphous phase arising from the homogeneous mixing of the nylon 6 and POP segments.

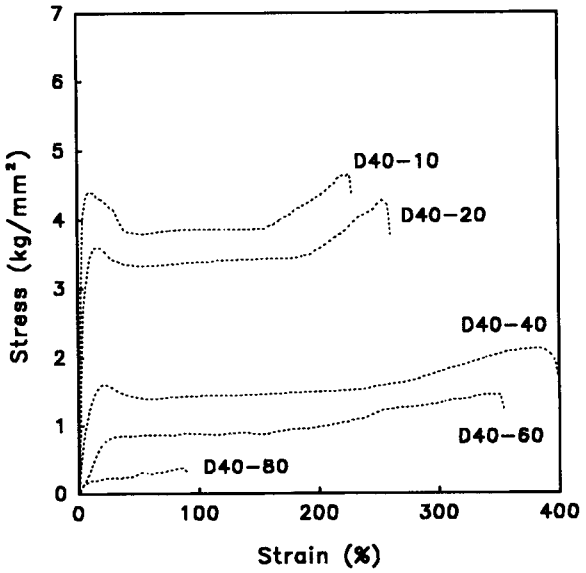

Figure 16 Strain–stress curves for nylon 6–D40 copolymers.

The strain–stress curves of the nylon 6–D4 copolymers exhibit the characteristics of a plasticized thermoplastic.

On the other hand, it is assumed from the results of the DSC and dynamic mechanical analysis that the nylon 6–D20 and nylon 6–D40 copolymers having longer soft segments show the three-phase structures of a crystalline nylon 6 phase, an amorphous nylon 6–rich phase, and an amorphous POP-rich domain. The incorporation of longer soft segments into the nylon 6 backbone induced a better phase separation and enhanced the purity of the hard and soft domains as well as the crystal perfectness. The nylon 6–D20 copolymers showed better elastic properties as the soft segment content increased. However, the nylon 6–D40 copolymers did not give good elastic properties due to high interconnectivity of the hard domain, and their mechanical properties became worse because of the lack of crosslinking density as the soft-segment content increased.

REFERENCES

1. G. Deleens, P. Foy, and E. Marechal, *Eur. Polym. J.*, **13,** 337 (1977).
2. L. Castaldo, G. Maglio, and R. Palumbo, *J. Polym. Sci., Polym. Lett. Ed.*, **16,** 643 (1978).
3. S. Mumcu, K. Burzin, R. Feldmann, and R. Feinauer, *Angew. Makromol. Chem.*, **74,** 49 (1978).
4. R. J. Gaymans, P. Schwering, and J. L. de Haan, *Polymer,* **30,** 974 (1989).
5. P. F. van Hutten, E. Walch, A. H. M. Veeken, and R. J. Gaymans, *Polymer,* **31,** 524 (1990).
6. T. Otsuki, M. Kakimoto, and Y. Imai, *J. Appl. Polym. Sci.,* **40,** 1433 (1990).
7. Z. G. Gardlund and M. A. Bator, *J. Appl. Polym. Sci.,* **40,** 2027 (1990).
8. D. J. Sikkema, *J. Appl. Polym. Sci.,* **43,** 877 (1991).
9. Y. C. Yu and W. H. Jo, *J. Appl. Polym. Sci.,* **54,** 585 (1994).
10. Y. P. Chang and G. L. Wilkes, *J. Polym. Sci., Polym. Phys. Ed.,* **13,** 455 (1975).
11. E. Sorta and A. Melis, *Polymer,* **19,** 1153 (1978).
12. F. G. Schmid and M. Droscher, *Makromol. Chem.,* **184,** 2669 (1983).
13. J. Blackwell and C. D. Lee, *J. Polym. Sci., Polym. Phys. Ed.,* **22,** 759 (1984).
14. J. T. Koberstein and A. F. Galambos, *Macromolecules,* **25,** 759 (1984).
15. T. Arakawa and F. Nagatoshi, *J. Polym. Sci., A-2,* **7,** 1461 (1969).
16. M. Todoki and T. Kawaguchi, *J. Polym. Sci., Polym. Phys. Ed.,* **15,** 1067 (1977).
17. J. P. Bell and J. H. Dumbleton, *J. Polym. Sci., A-2,* **7,** 1033 (1969).
18. F. J. Hybart and L. D. Platt, *J. Polym. Sci.,* **11,** 1449 (1967).
19. J. A. Miller, S. B. Lin, K. K. S. Hwang, K. S. Wu, P. E. Gibson, and S. L. Cooper, *Macromolecules,* **18,** 32 (1985).
20. D. J. Skrovanek, P. C. Painter, and M. M. Coleman, *Macromolecules,* **18,** 1676 (1985).
21. D. J. Skrovanek, P. C. Painter, and M. M. Coleman, *Macromolecules,* **19,** 699 (1986).
22. M. Beer, H. B. Kessler, and G. B. B. M. Sutherland, *J. Chem. Phys.,* **29,** 1097 (1958).
23. L. G. Roldan, F. Rahl, and A. R. Paterson, *J. Polym. Sci., Part C,* **8,** 145 (1965).
24. J. F. Beecher, L. Marker, R. D. Bradford, and S. L. Aggarwal, *J. Polym. Sci., Part C,* **26,** 117 (1969).
25. Richard J. Cella, *J. Polym. Sci.: Symposium,* **42,** 727 (1973).

Received April 19, 1994
Accepted June 23, 1994